

SCIENTIFIC REPORTS

OPEN

Distinctive effect on nerve growth factor-induced PC12 cell neurite outgrowth by two unique neolignan enantiomers from *Illicium merrillianum*

Received: 24 June 2015
Accepted: 22 October 2015
Published: 20 November 2015

Xinhui Tian¹, Rongcai Yue², Huawu Zeng¹, Honglin Li³, Lei Shan¹, Weiwei He³, Yunheng Shen¹ & Weidong Zhang^{1,2}

Merrillianoid (**1**), a racemic neolignan possessing the characteristic benzo-2,7-dioxabicyclo[3.2.1]octane moiety, was isolated from the branches and leaves of *Illicium merrillianum*. Chiral separation of **1** gave two enantiomers (+)-**1** and (–)-**1**. The structure of **1** was established by comprehensive spectroscopic analysis and single crystal X-ray diffraction. The absolute configurations of enantiomers were determined by quantum mechanical calculation. Compound (+)-**1** exhibited a better neurotrophic activity than racemate **1** by promoting nerve growth factor (NGF) induced PC12 cell neurite outgrowth, while (–)-**1** showed a distinctive inhibitory effect. Furthermore, a mechanism study indicated that the two enantiomers influenced NGF-induced neurite outgrowth of PC12 cells possibly by interacting with the trkA receptor, and extracellular signal regulated kinases 1/2 (ERK1/2) and mitogen-activated protein kinase (MEK) in Ras/ERK signal cascade. But the phosphorylation level of serine/threonine kinase Akt1 and Akt2 in PI3K/Akt signal pathway showed no significant difference between (+)-**1** and (–)-**1**.

Nerve growth factor (NGF) is the first member of neurotrophin, it acts on sympathetic and sensory neurons and functions as a trophic factor for distinct populations of neurons in central nervous system¹. The depletion of NGF has been linked with neurodegenerative disorders such as Alzheimer's disease², while over expression of it is related with other diseases such as epilepsy³, glioma⁴, tumor metastasis^{5,6} etc. Thus small-molecular neurotrophin agonist or antagonist is of high interest to promote or inhibit NGF activity. To find NGF agonist or antagonist activity compounds, we made use of rat pheochromocytoma-derived PC12 cells as a model system. In response to NGF, PC12 cells differentiate into sympathetic-like neurons and extend long neurites, providing a useful model for the investigation of neuronal differentiation, signaling and other neurobiological events⁷.

The functions of NGF are mediated by high-affinity tyrosine kinase receptor type 1 (TrkA) and the low-affinity non-enzymatic p75 neurotrophin receptor (P75^{NTR})⁸. Activation of trkA mediates neurite outgrowth and neuronal survival, whereas p75^{NTR} induces apoptosis in some neuron cells. Evidence suggests that NGF binding to TrkA leads to the activation of Ras/ERK and PI3K/Akt downstream pathways⁹. Since the two pathways are critical for NGF-induced neuronal differentiation and survival of PC12

¹Department of Phytochemistry, School of Pharmacy, Second Military Medical University, 325 Guohe Road, Shanghai 200433, P. R. China. ²School of Pharmacy, Shanghai Jiao Tong University, 800 Dongchuan Road, Shanghai 200240, P. R. China. ³School of Pharmacy, East China University of Science and Technology, 130 Meilong Road, Shanghai 200237, P. R. China. Correspondence and requests for materials should be addressed to Y.S. (email: shenyunheng@hotmail.com) or W.Z. (email: wdzhangy@hotmail.com)

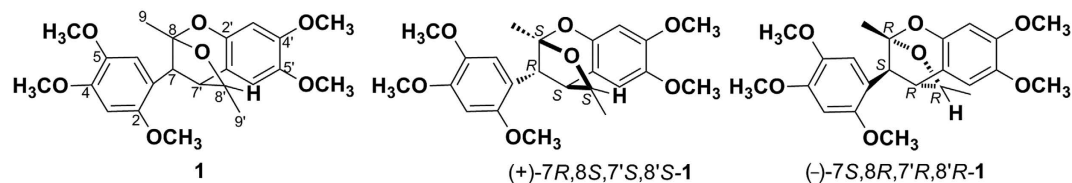


Figure 1. The chemical structures of **1**, (+)-**1** and (–)-**1**.

cells^{10,11}, we investigated the influence of compounds on the phosphorylation of associated proteins in Ras/ERK and PI3K/Akt pathway.

Natural products are rich sources of lead compounds for drug discovery due to their unique structure and bioactivities¹². For example, neurotrophic 11-*O*-debenzoyltashironin¹³, (–)-hinokinin^{14,15} and merrillactone A¹⁶ with unique structure had been isolated from the pericarps of *Illicium merrillianum*. *I. merrillianum* is a shrub or small tree indigenous to southwestern China and Burma, and locally used as an antirheumatic agent¹⁷. In our continuous effort to find new bioactive natural products from *I. merrillianum*, we have previously reported a novel isopropyl (13 → 11)-*abeo*-9,11-*seco* abietane diterpenoid and six other abietane diterpenoids¹⁸.

In this study, merrillianoid (**1**), a racemic neolignan possessing unique benzo-2,7-dioxabicyclo[3.2.1]octane moiety was isolated from the branches and leaves of *I. merrillianum*, and chiral separation of **1** gave two enantiomers (+)-**1** and (–)-**1** (Fig. 1). Biological assay revealed that (+)-**1** had a better effect than racemate **1** in promoting NGF-induced PC12 cell neurite outgrowth at concentrations of 1–10 μM, while (–)-**1** showed quite distinctive inhibitory effect also at concentrations as low as 1 μM. Moreover, a mechanism study indicated that the two enantiomers exerted their promoting or inhibitory activities possibly by regulating the phosphorylation of TrkA receptor, the extracellular signal regulated kinases 1/2 (ERK1/2), and mitogen-activated protein kinase (MEK) in Ras/ERK pathway. However the phosphorylation level of serine/threonine kinase Akt1 and Akt2 in PI3K/Akt pathway showed no significant difference between (+)-**1** and (–)-**1**. These findings provided a pair of interesting neolignans for NGF-agonist and antagonist drug design, and revealed that absolute configurations dramatically affected biological activities of compounds.

Results and Discussion

Compound **1** was obtained as colorless needle crystal. The IR spectrum displayed absorptions due to the C–O bands at 1033, 1203 cm^{−1}, and the phenyl groups at 1464, 1508 cm^{−1}. The HRESIMS spectrum gave a pseudo-molecular-ion peak [M + H]⁺ at *m/z* = 417.1915 (calcd. 417.1913), which corresponding to a molecular formula C₂₃H₂₉O₇ with ten degrees of unsaturation.

The ¹H NMR spectrum of **1** displayed four singlet aromatic protons at δ_H = 6.39, 6.45, 6.46, 6.86 ppm, and one methyl and five methoxy groups at δ_H = 1.65, 3.55, 3.74, 3.77, 3.83, 3.85 ppm. Furthermore, the –CHCH₃ fragment was identified owing to the doublet methyl resonance at δ_H = 1.36 ppm (d, 3H, *J* = 6.5 Hz) and the quartet proton resonance at δ_H = 4.49 ppm (q, 1H, *J* = 6.5 Hz). An interpretation of the ¹³C and DEPT NMR spectra of **1** revealed 22 signals attributable to 23 carbon atoms, including nine quaternary carbon atoms (δ_C = 152.3, 148.9, 147.9, 146.5, 143.1, 142.5, 117.9, 115.2, 106.0 ppm), seven methine groups (δ_C = 112.6, 110.9, 100.3, 96.8, 85.2, 47.9, 38.9 ppm), and seven methyl groups (δ_C = 56.4, 56.2, 56.1, 56.0, 22.6, 20.7 ppm). The above ¹H, ¹³C and DEPT NMR spectroscopic data suggested that there were two 1,2,4,5-tetrasubstituted phenyl groups in **1**, and some of the resonances were quite similar to those of lignanoids.

More detailed information about the structure of **1** came from the interpretation of ¹H-¹H COSY, HSQC, HMBC, and NOESY spectra (Fig. 2). The HMBC correlations from 2-OCH₃ (δ_H = 3.83 ppm) to C-2 (δ_C = 147.9 ppm), 4-OCH₃ (δ_H = 3.85 ppm) to C-4 (δ_C = 152.3 ppm), and 5-OCH₃ (δ_H = 3.55 ppm) to C-5 (δ_C = 142.5 ppm), confirmed the primary locations of three methoxy groups. In the NOESY spectrum of **1**, the correlations between 3-H (δ_H = 6.46 ppm) and 2-OCH₃, 4-OCH₃, 6-H (δ_H = 6.86 ppm) and 5-OCH₃, 4-OCH₃ and 5-OCH₃ were observed. The above NOESY correlations, together with the key HMBC correlations from 3-H and 6-H to C-1 (δ_C = 115.2), C-2, C-4, and C-5, confirmed the presence of the first 1,2,4,5-tetrasubstituted phenyl group in **1**. Furthermore the HMBC correlations of 7-H (δ_H = 3.82 ppm) with C-1, C-2, and C-6 (δ_C = 112.6 ppm), and 9-CH₃ (δ_H = 1.65 ppm) with C-7 (δ_C = 38.9 ppm) and C-8 (δ_C = 106.0 ppm) assigned the C7-C8-C9 side chain to C-1, establishing phenyl propane unit **A**. The HMBC correlations from 4'-OCH₃ (δ_H = 3.77 ppm) to C-4' (δ_C = 148.9 ppm), and 5'-OCH₃ (δ_H = 3.74 ppm) to C-5' (δ_C = 143.1 ppm), confirmed the primary locations of another two methoxy groups. The NOESY correlations between 3'-H (δ_H = 6.45 ppm) and 4'-OCH₃, 6'-H (δ_H = 6.39 ppm) and 5'-OCH₃, 4'-OCH₃ and 5'-OCH₃ were observed, the above correlations, together with the HMBC correlations from 3'-H and 6'-H to C-1' (δ_C = 117.9 ppm), C-2' (δ_C = 146.5 ppm), C-4' and C-5' confirmed the presence of another 1',2',4',5'-tetrasubstituted phenyl group in **1**. The HMBC correlations of 7'-H (δ_H = 3.03 ppm) with C-1', C-2', and C-6' (δ_C = 110.9 ppm), and 9'-CH₃ (δ_H = 1.36 ppm) with C-7' (δ_C = 47.9 ppm) and C-8' (δ_C = 85.2 ppm) assigned the C7'-C8'-C9' side chain to C-1', and established

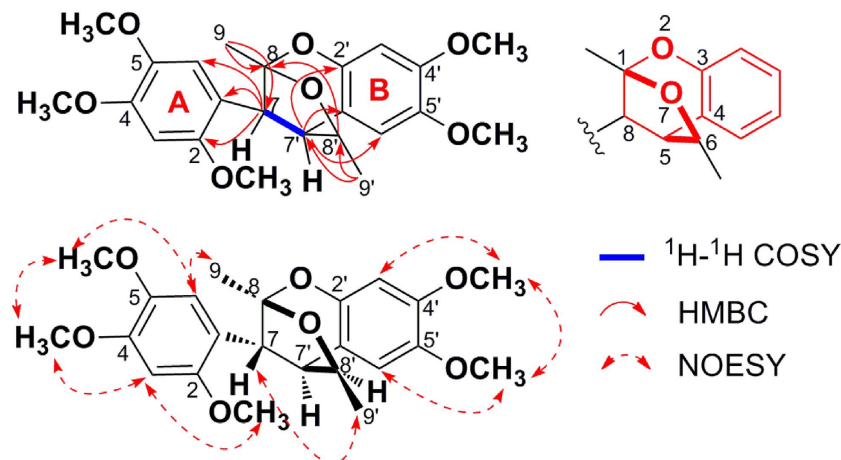


Figure 2. Key ^1H – ^1H COSY, HMBC, and NOESY correlations of **1**.

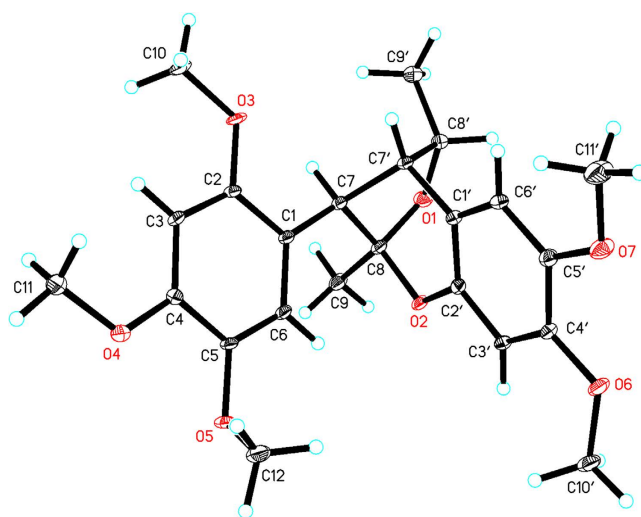


Figure 3. Single crystal X-ray diffraction of **1**.

phenyl propane unit **B**. A spin coupling system H-7/H-7' was established by the ^1H - ^1H COSY spectrum, which indicated that phenyl propane units **A** and **B** were connected by C(7')-C(7) bond. The HMBC cross-peak from 8'-H ($\delta_{\text{H}} = 4.49$ ppm) to C-8, suggesting the existence of an ether bridge between C-8' and C-8, forming a tetrahydrofuran ring. Deducting nine degrees of unsaturation accounted for two 1,2,4,5-tetrasubstituted phenyl groups and one tetrahydrofuran ring, the remaining one degree of unsaturation suggested that an additional ring was required. On the basis of the chemical shift, C-8 was supposed to link to C-2' through an oxygen atom. Thus, the structure of **1** was established as depicted, and named merrillianoid, which possessed unique structure featured with a ketal formed between C-8 and C-2', C-8', forming a characteristic benzo-2,7-dioxabicyclo[3.2.1]octane moiety (Fig. 1). The proposed structure was further supported by the fragment ions at m/z 439 $[\text{M} + \text{Na}]^+$, 247, 203 in the MS, MS², MS³ spectra of **1** (see supporting information Fig. S1, S2).

In the NOESY spectrum of merrillianoid (**1**), the correlations of 9'-CH₃ with 7-H, and 9-CH₃ with 6-H established the relative configuration of **1**. The single crystal X-ray diffraction (Cu-K α radiation; CCDC number: 1055836) further confirmed the relative configuration of **1** (Fig. 3). However, the space group $P2_1/c$ of **1** was achiral, which was an indicative of its racemic nature. The lack of optical activity further confirmed that **1** was racemic. Subsequent HPLC separation of **1** on a chiral column led to two enantiomers (+)-**1** and (-)-**1**, which had opposite optical rotation and Cotton effects (see supporting information Fig. S7, S8). However, the single crystals of either of the two optically pure enantiomers can not be obtained in several solvent systems.

Recently, quantum mechanical computation of electronic circular dichroism (ECD) has been successfully applied to determine the absolute configurations of natural products^{19,20}. To determine the absolute configurations of the two enantiomers, we compared the experimentally observed CD spectra of

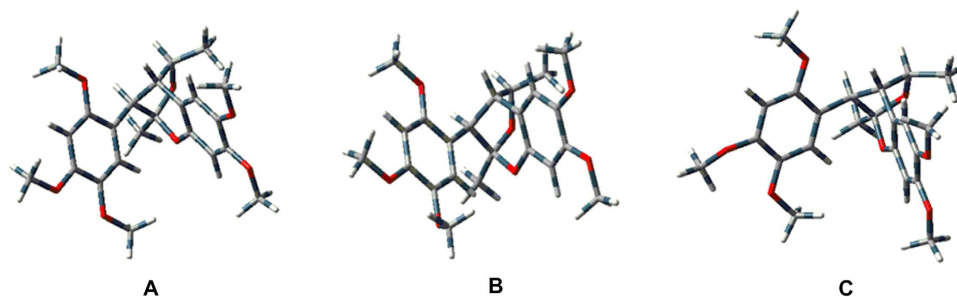


Figure 4. Optimized geometries of (+)-**1** (A–C) at the B3LYP/3-21G level.

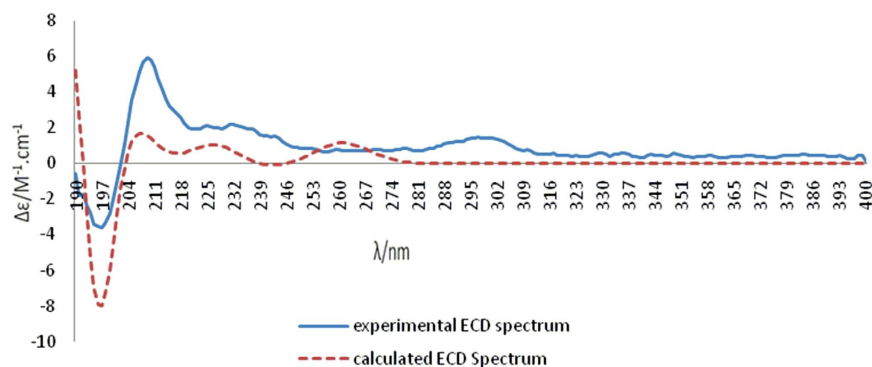


Figure 5. Experimental CD spectrum of (+)-**1** and the calculated ECD spectrum of (7*R*,8*S*,7'*S*,8'*S*)-**1** in methanol at the B3LYP/3-21G level with the PCM model.

(+)-**1** and (–)-**1** with the calculated ECD spectra obtained by quantum mechanical computation with the Gaussian03 software (Revision E.03. [Gaussian, Inc. (ed)] (Wallingford CT, USA, 2004)). Because of the rigid structure of **1** and the relative configuration established by NOESY experiment and single crystal X-ray diffraction, the arbitrarily assigned absolute configuration of 7*R*,8*S*,7'*S*,8'*S* for (+)-**1** was geometrically optimized by using density functional theory (DFT) at B3LYP/3-21G level to afford three preferred conformers A–C ($\Delta E < 5.0$ kJ/mol) (Fig. 4). The ECD spectra of conformers A–C was then calculated at the B3LYP/3-21G level in the methanol solution with the PCM model. Each calculated ECD spectrum was assigned a Boltzmann weight according to the energy of the minimized conformers at 298.15 K and overlaid to give the calculated ECD spectrum. As depicted in Fig. 5, the calculated ECD spectrum for (7*R*,8*S*,7'*S*,8'*S*)-**1** matched well with the experimentally measured CD spectrum of (+)-**1**, which showed negative Cotton effects at 190–200 nm, and positive Cotton effects at 204–218 nm. Thus the absolute configuration of (+)-**1** was assigned as 7*R*,8*S*,7'*S*,8'*S*. Similarly, the absolute configuration of (–)-**1** was determined to be 7*S*,8*R*,7'*R*,8'*R* by the same method as (+)-**1** (see supporting information Fig. S6, S8).

The NGF-mediated neurotrophic activity of enantiomers (+)-**1** and (–)-**1**, and racemate **1** were evaluated using rat pheochromocytoma (PC12) cells as a model system of neuronal differentiation²¹. As shown in Fig. 6A, all compounds at concentrations of 0.1–10 μ M had no cytotoxic activity against PC12 cells by MTT assay. Then we further studied their effects on neurite outgrowth of PC12 cells (Fig. 6B,C). The mean value was expressed as percent of neurite-bearing cells in samples treated with compounds with or without 20 ng/mL NGF. The results showed that all compounds didn't morphologically affect neurite outgrowth of PC12 cells in the absence of NGF. However, when in the presence of 20 ng/mL NGF, racemate **1** significantly increased PC12 cell differentiation rates (21.48 \pm 0.71% at 1 μ M, 26.40 \pm 0.63% at 10 μ M, $P < 0.01$), comparing with 20 ng/mL NGF alone (18.22 \pm 1.53%, $P < 0.01$). Enantiomer (+)-**1** had a better promoting effect than racemate **1** with differentiation rates of 28.05 \pm 0.71% at 1 μ M, 35.47 \pm 1.40% at 10 μ M ($P < 0.01$), while (–)-**1** exhibited a distinctive inhibitory effect with neuronal differentiation rates of 17.05 \pm 0.71% at 1 μ M, and 14.47 \pm 1.40% at 10 μ M ($P < 0.01$). Overall, despite having the same planar structure, the opposite absolute configurations for (+)-**1** and (–)-**1** resulted in distinctive effects on NGF-induced PC12 cell differentiation.

We further investigated the possible molecular mechanism of merrillianoids on NGF-induced PC12 cell differentiation by western blotting analysis²². Since trkA receptor activation leads to the phosphorylation of extracellular signal-regulated protein kinase 1/2 (ERK1/2) via mitogen-activated protein kinase (MEK) in the process of neurite outgrowth of PC12 cells²³, we investigated the influences of these compounds on the phosphorylation of TrkA, MEK and ERK1/2 during the NGF-induced neurite outgrowth

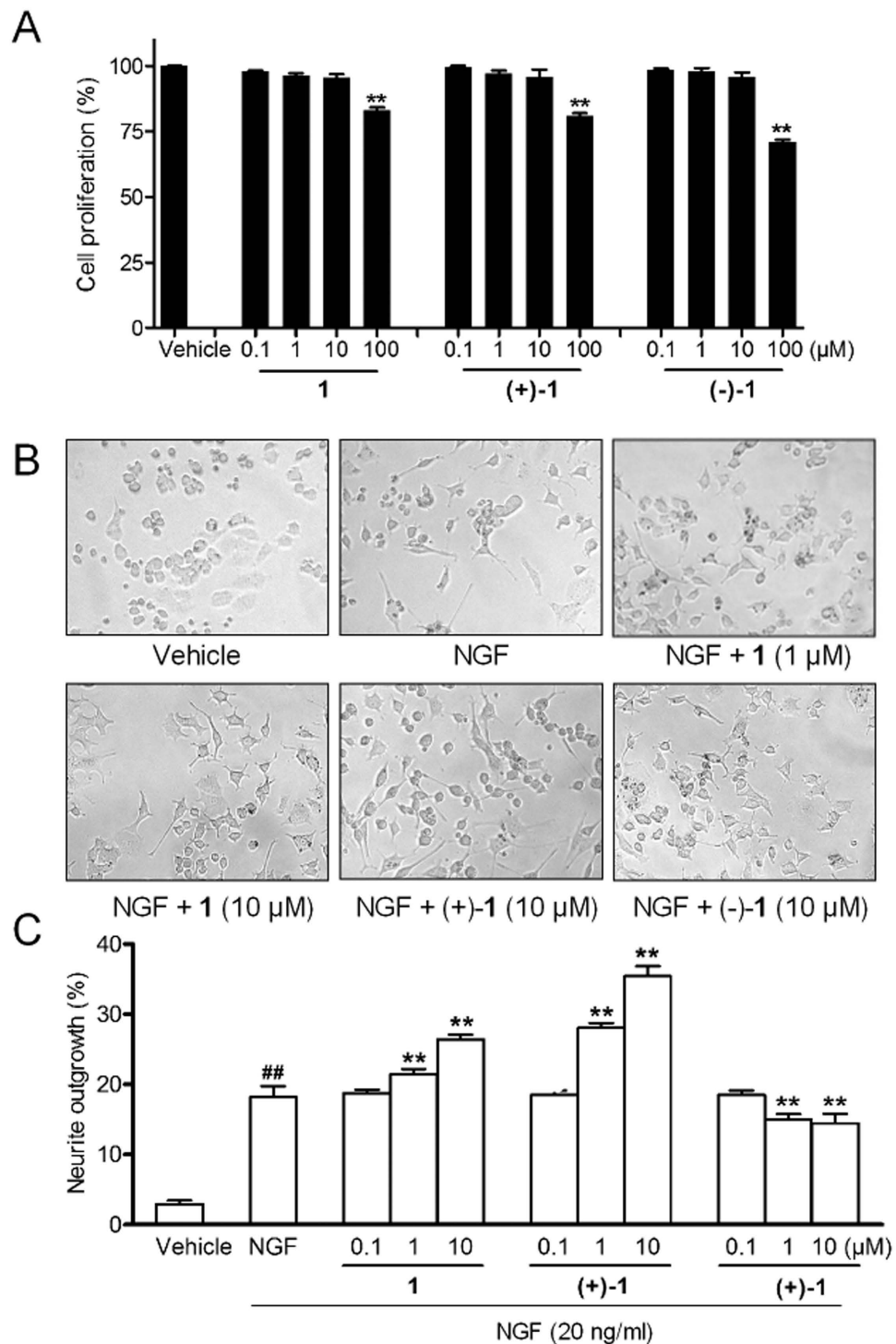


Figure 6. (A) PC12 cells proliferation after exposure to 0.1% DMSO or serial concentrations of **1**, (+)-**1** and (-)-**1**, for 24 h. (B) Representative images of the effects of **1**, (+)-**1**, and (-)-**1** on NGF-induced neurite outgrowth of PC12 cells. (C) Effects of **1**, (+)-**1**, and (-)-**1** on NGF-induced neurite outgrowth of PC12 cells at 0.1, 1, and 10 μM (Values were considered as significant at: ## $P < 0.01$ vs. vehicle, ** $P < 0.01$ vs. 20 ng/mL NGF).

of PC12 cells (Fig. 7A). Treatment of PC12 cells with NGF (20 ng/mL) induced the phosphorylation of TrkA, MEK and ERK1/2 for 30 min. The relative phosphorylation level of TrkA, MEK and ERK1/2 of **1** and (+)-**1** both increased significantly comparing to 20 ng/mL NGF (0.70 ± 0.037 for TrkA, 0.76 ± 0.107 for MEK, 0.92 ± 0.048 for ERK1/2), and the phosphorylation level of (+)-**1** at 10 μM (2.13 ± 0.052 for TrkA, 1.99 ± 0.030 for MEK, 4.40 ± 0.179 for ERK1/2) was higher than that of racemate **1** (1.23 ± 0.174

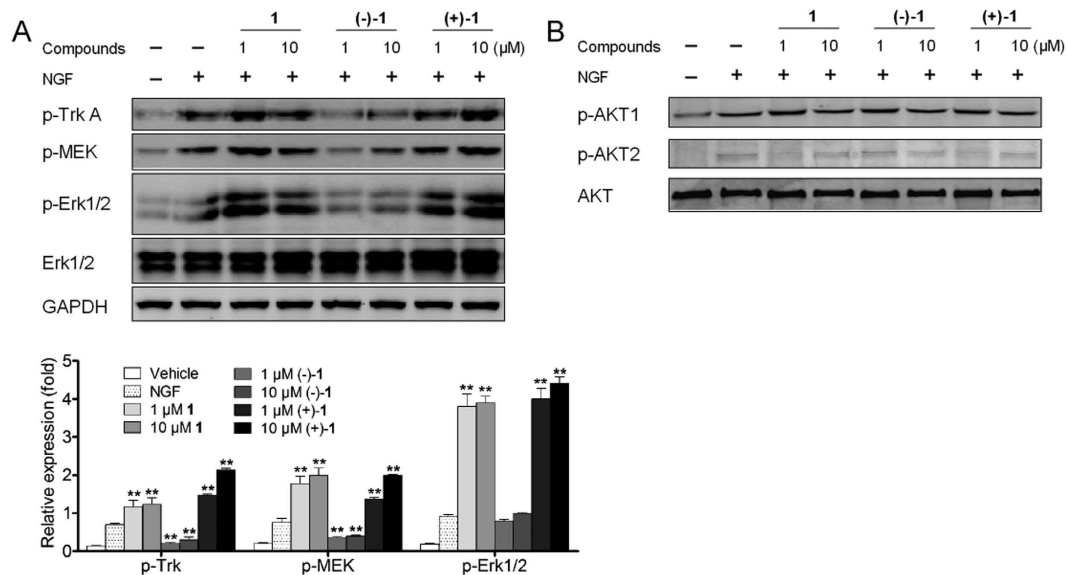


Figure 7. Western blotting analysis after 30 min treatment of PC12 cells with **1**, (+)-**1**, and (-)-**1** in NGF-induced TrkA, MEK, ERK1/2, Akt1, and Akt2 phosphorylation as indicated. Data shown are the results of three different experiments and are represented as the relative densities of protein bands normalized to GAPDH (** $P < 0.01$ vs. vehicle).

for TrkA, 1.90 ± 0.202 for MEK, 3.90 ± 0.052 for ERK1/2). The phosphorylation level of (+)-**1** and **1** was in proportion to their neurite outgrowth promoting activities. As for (-)-**1**, the relative ratio of p-TrkA, and p-MEK decreased dramatically (0.30 ± 0.074 for TrkA, 0.40 ± 0.020 for MEK at $10 \mu\text{M}$) comparing with 20 ng/mL NGF. In a word, compound (+)-**1** promoted the NGF-induced neurite outgrowth of PC12 cells by enhancing the phosphorylation level of TrkA receptor, and MEK, ERK1/2 in Ras/ERK signaling pathway, while (-)-**1** inhibited neurite outgrowth of PC12 cells via suppressing the phosphorylation of the above proteins.

The PI3K/Akt signaling cascade regulated cell survival and suppress apoptosis in a wide range of neuronal cell types^{10,24,25}. Thus we detected the influence of all compounds on the phosphorylation of Akt-related serine/threonine kinase Akt1 and Akt2 during the NGF-induced PC12 cell differentiation. The western blotting analysis showed that there was no significant difference between all trial groups in the phosphorylation level of Akt1 and Akt2 (Fig. 7B).

In conclusion, two neolignan enantiomers (+)-**1** and (-)-**1** with characteristic benzo-2,7-dioxabicyclo[3.2.1]octane moiety were isolated from the branches and leaves of *I. merrillianum*. The kind of neolignans with benzo-2,7-dioxabicyclo[3.2.1]octane bridged-ring was first encountered in nature. Moreover (+)-**1** was found to have a better effect than racemate **1** in promoting NGF-induced neurite outgrowth of PC12 cells possibly by increasing the phosphorylation level of TrkA receptor, and MEK, ERK1/2 in Ras/ERK signaling cascade at concentrations of $1\text{--}10 \mu\text{M}$, while its enantiomer (-)-**1** played the opposite role at the same concentrations. Opposite absolute configuration leads to big difference between the interaction of compounds and the PC12 cells. However the phosphorylation level of Akt1 and Akt2 in the PI3K/Akt pathway showed no significant differences between (+)-**1** and (-)-**1**. The results reported in this paper offer a pair of interesting neolignan enantiomers for potential NGF agonist and antagonist drug development.

Materials and Methods

General. 1D and 2D NMR spectra were recorded on a Bruker Ascend 500 NMR spectrometer with TMS as internal standard; ESIMS, MS², and MS³ were measured on the Agilent LC/MSD Trap XCT spectrometer and HRESIMS were performed on an Agilent 6520 Accurate-MS Q-TOF LC/MS system; Optical rotations were obtained with an Autopol VI (Rudolph Research Analytical, Hackettstown, NJ); CD spectra were recorded on a Chirascan spectrometer (Applied Photophysics, UK); IR spectrum was acquired with a Bruker Vector-22 spectrometer with KBr pellets; Colum chromatography was performed on silica gel (80–100 mesh, Huiyou Silica Gel Development Co., Ltd. Yantai, China); Reversed phase medium pressure liquid chromatography (RP-MPLC) was performed on a Buchi Sepacore system; TLC analysis was run on HSGF₂₅₄ silica gel plates ($1\text{--}40 \mu\text{m}$, Huiyou Silica Gel Development Co., Ltd. Yantai, China); Preparative TLC was conducted with pre-coated silica gel HSGF₂₅₄ plate (Huiyou Silica Gel Development Co., Ltd. Yantai, China).

Plant Material. The branches and leaves of *I. merrillianum* were collected in Gongshan county, Yunnan province, P. R. China, in August 2011, and authenticated by Prof. Han-Ming Zhang of Second Military Medical University. A voucher specimen (No. 20110815) is deposited in the School of Pharmacy, Second Military Medical University.

Extraction and Isolation. The air-dried and chopped branches and leaves of *I. merrillianum* (20 kg) were extracted with 95% EtOH (3 × 80 L) for three times (3 × 1 hr) to afford a crude extract (1.7 kg) after removal of solvent under low pressure. The extract was suspended in water and partitioned with petroleum ether (488 g), EtOAc (836 g), and *n*-BuOH (526 g) successively. The petroleum ether extract was subjected to silica gel column chromatography (CC) (3.4 kg, 80–100 mesh), using petroleum ether-EtOAc gradient elution (50:1–0:1) to afford seven fractions A (51 g), B (86 g), C (95 g), D (16 g), E (21 g), F (129 g), G (17 g). Fraction F was subjected to RP-MPLC (MeOH/H₂O, 40–100%) to give five fractions F-1 (30 g), F-2 (21 g), F-3 (15 g), F-4 (31 g), F-5 (13 g). Fraction F-5 was further subjected to RP-MPLC (MeOH-H₂O, 40–100%) to give five fractions (F-51, F-52, F-53, F-54, F-55). Compound **1** (14.8 mg) was isolated from fraction F-53 by applying preparative TLC using petroleum ether-Me₂O (3:1, *R_f* = 0.43) developer.

Chiral separation of 1. HPLC chiral separation of **1** was performed on a Chiralpak IA column (USA): 0.46 cm I.D. × 25 cm; Flow rate: 1.0 mL/min; Solvent: Hexane/DCM/DEA = 45/55/0.1 (v/v/v); Temperature: 30 °C; Wavelength: 254 nm; Injection volume: 10 μL for each sample; The retention time of (+)-**1** (4.0 mg) and (–)-**1** (5.0 mg) was 7.935 and 8.635 min, respectively, and the peak area ratio of (+)-**1** to (–)-**1** was 0.8:1 (Fig. S4).

Merrillianoid (1). colorless needle crystal (MeOH); mp. 58 ~ 59 °C; [α]_{25 D} of (+)-**1**: + 48.0 (c 0.25, MeOH), [α]_{25 D} of (–)-**1**: –48.0 (c 0.25, MeOH); CD of (+)-**1** (c 1.00 mmol/L, CH₃OH, 25 °C) nm ($\Delta\epsilon$) 197 (–3.5), 210 (+5.8), CD of (–)-**1** (c 1.00 mmol/L, CH₃OH, 25 °C) nm ($\Delta\epsilon$) 197 (+3.5), 210 (–5.8); IR (KBr) ν_{\max} 2935, 1618, 1508, 1465, 1204, 1034, 884 cm^{–1}; HRESIMS *m/z* 417.1915 [M + H]⁺ (calcd. for C₂₃H₂₉O₇, 417.1913); ¹H-NMR (500 MHz, CDCl₃) δ : 1.36 (3H, d, *J* = 6.5 Hz, H-9'), 1.65 (3H, s, H-9), 3.03 (1H, d, *J* = 3.5 Hz, H-7'), 3.55 (3H, s, OCH₃-5), 3.74 (3H, s, OCH₃-5'), 3.77 (3H, s, OCH₃-4'), 3.82 (1H, m, H-7), 3.83 (3H, s, OCH₃-2), 3.85 (3H, s, OCH₃-4), 4.49 (1H, q, *J* = 6.5 Hz, H-8'), 6.39 (1H, s, H-6'), 6.45 (1H, s, H-3'), 6.46 (1H, s, H-3), 6.86 (1H, s, H-6); ¹³C-NMR (125 MHz, CDCl₃) δ : 115.2 (C-1), 147.9 (C-2), 96.8 (C-3), 152.3 (C-4), 142.5 (C-5), 112.6 (C-6), 38.9 (C-7), 106.0 (C-8), 22.6 (C-9), 117.9 (C-1'), 146.5 (C-2'), 100.3 (C-3'), 148.9 (C-4'), 143.1 (C-5'), 110.9 (C-6'), 47.9 (C-7'), 85.2 (C-8'), 20.7 (C-9'), 56.1 (OCH₃-2), 56.2 (OCH₃-4), 56.0 (OCH₃-4', 5), 56.4 (OCH₃-5').

Computational Details. The theoretical calculations of (+)-**1** and (–)-**1** were performed on an IBM cluster machine using Gaussian03 package. Conformational analysis for 7*R*,8*S*,7'*S*,8'*S*-**1** and 7*S*,8*R*,7'*R*,8'*R*-**1** was initially carried out via the Molecular Operating Environment (MOE) software package using the MMFF94 force field. The obtained conformers were further optimized, and verified as the true minima of potential energy surface using TDDFT at B3LYP/3-21G(d) basis set level. Conductor-like polarizable continuum model (CPCM) was adopted to consider solvent effects using the dielectric constant of methanol (ϵ = 32.6). The 21 lowest electronic transitions were calculated and the rotational strengths of each electronic excitation were given using both dipole length and dipole velocity representations. ECD spectra were stimulated using a Gaussian function with a half-bandwidth of 0.3 eV. Equilibrium populations of conformers at 298.15 K were calculated from their relative free energies (ΔG) using Boltzmann statistics. The overall ECD spectra of (+)-**1** and (–)-**1** were then generated according to Boltzmann weighting of each conformers.

Conformational analysis. Conformational analysis was initially carried out using Maestro7.5 conformational searching, together with the MMFF94 molecular mechanics methods. MMFF94 structures were reoptimized using ab initio DFT at the B3LYP/3-21G (d) level. Energy of stable conformations were calculated and led to the relative energy, which in turn allowed the room temperature equilibrium populations to be calculated according to Maxwell - Boltzmann distribution law (Eqn 1).

$$\frac{N_i}{N} = \frac{g_i \exp(-E_i/kT)}{\sum_j g_j \exp(-E_j/kT)} \quad (1)$$

Original ECD data calculations. Excitation energy (in nm) and rotatory strength *R* (velocity form *R*^{vel} and length form *R*^{len} in 10^{–40} erg-esu-cm/Gauss) between different states were calculated by time dependant density functional theory (TDDFT) at B3LYP/3-21G (d)//B3LYP/3-21G (d) level in methanol solution. All calculations are performed by the Gaussian03 program package.

ECD simulation. The ECD spectra were then simulated by overlapping Gaussian functions for each transition according to Eqn 2:

$$\Delta \in (E) = \frac{1}{2.297 \times 10^{-39}} \frac{1}{\sqrt{2\pi}\sigma} \sum_i^A \Delta E_i R_i e^{-[(E-\Delta E_i)/(2\sigma)]^2} \quad (2)$$

where σ is the width of the band at 1/e height and ΔE_i and R_i are the excitation energies and rotatory strengths for transition i , respectively, $\sigma = 0.30$ eV and R^{rel} have been used in this work. Conformational analysis has been carried out and theoretically weighted ECD spectra have been simulated at different levels mentioned above.

Chemicals and Reagents for Biological activities. The undifferentiated rat pheochromocytoma cells line (PC12) were obtained from the Cell Bank of Shanghai Institute of Biochemistry & Cell Biology, Shanghai Institute for Biological Sciences, Chinese Academy of Sciences; NGF was purchased from Wuhan Hiteck Biological Pharma Co., Ltd. China; Dimethylsulfoxide (DMSO) and [3-(4,5-dimethylthiazol-2-yl)-2,5-diphenyltetrazolium bromide] (MTT) were purchased from Sigma (St. Louis, Mo., USA); Dulbecco's Modified Eagle's Medium (DMEM), a penicillin/streptomycin mixture, and fetal calf serum (FCS) and horse serum (HS) were purchased from Gibco (Grand Island, New York); Antibodies for p-TrkA, p-MEK, p-ERK1/2, p-Akt1 (Ser473), p-Akt2 (Thr308) and ERK1/2, Akt were obtained from Cell Signaling Technology (Beverly, MA); Anti-mouse and anti-rabbit secondary antibody were purchased from Odyssey (Li-Cor Biosciences, Lincoln, NE, USA); GAPDH (glyceraldehyde-3-phosphate dehydrogenase) was purchased from Beyotime Biotechnology (Jiangsu, China).

MTT assay. The assay was performed in triplicate. PC12 cells were maintained in DMEM containing 5% FCS and 10% HS supplemented with 100 U/mL penicillin and 100 μ g/mL streptomycin in a humidified atmosphere containing 5% CO₂ at 37°C. The tested compounds were dissolved in DMSO, and the final volume for DMSO in each well was no more than 0.1%. To rule out a potential influence of the solvent, we conducted a corresponding control experiments. PC12 cells were seeded in 96-well plate at a density of 5×10^4 /well. After cell attachment overnight, each well was treated with different concentrations of test compounds or 0.1% DMSO for 24 h. Then 10 μ L of MTT solution (5 mg/mL) was added to each well and the cultures were incubated for another 4 h at 37°C. The supernatant was then removed and 100 μ L of DMSO was added to each well and agitated at 60 rpm for 5 min to dissolve the precipitate. The absorbance was read at 570 nm by a SYNERGY microplate reader (BioTek, Winooski, VT).

Neurite outgrowth assay. Undifferentiated PC12 cells were plated in a density of 5×10^4 cells/well in the above medium in 96-well plate. After cell attachment overnight each well was treated with compounds with or without 20 ng/mL NGF respectively (NGF was dissolved in PBS, and its final volume was no more than 0.1%). After 24-h incubation, neurite outgrowth of the cells were determined by light microscopy (Leica DMI3000B, Nussloch, Germany). Neurite processes with a length equal to or greater than the diameter of the neuron cell body were scored as positive. Neurite outgrowth was determined from at least three different regions of interest in three independent experiments. Cell differentiation rate was calculated as the positive number of cells/total cell number. Data were expressed as the mean \pm standard deviation (SD).

Western blotting assay. PC12 cells were incubated at 37°C for 24 h in a density of 1×10^6 cells/well in six well palte. Then they were incubated with 20 ng/mL NGF and different concentrations of compounds for 30 min. After removal of the medium, PC12 cells were washed with ice-cold PBS, resuspended in lysis buffer containing 150 mM NaCl, 50 mM Tris (pH 8.0), 0.02% NaN₃, 0.01% PMSE, 0.2% Aprotinin, 1% TritonX-100 supplemented with protease inhibitor cocktail (Sigma, St. Louis, Mo.), and then centrifuged at 1,2000 rpm for 15 min. The concentration of total proteins was determined using a BCA kit (Pierce, Rockford, IL). After boiling for 5 min the protein samples (30 μ g) were electrophoresed on 10% SDS polyacrylamide gels and then transferred to polyvinylidene difluoride (PVDF) membrane. Nonspecific reactivity was blocked by 5% nonfat milk prepared in TBST (10 mM Tris, 150 mM NaCl, 0.05% Tween-20, pH 7.5) at room temperature for 1 h. The membranes were incubated with antibodies according to the manufacturers' instructions. The image was captured by the Odyssey infrared imaging system (Li-Cor Bioscience, Lincoln, NE). Protein densitometry was done using Quantity One imaging software (Bio-Rad) and normalized against GAPDH.

Statistical analysis. Data were analyzed using GraphPad Prism software (Graph Pad software Inc., San Diego, CA, USA). The comparison between two groups was analyzed by unpaired Student *t*-test, and multiple comparisons were compared by one-way ANOVA analysis of variance followed by Tukey post hoc test. Statistical significance was determined as $P < 0.05$.

References

- Shelton, D. L. & Reichardt, L. F. Studies on the expression of the β nerve growth factor (NGF) gene in the central nervous system: Level and regional distribution of NGF mRNA suggest that NGF functions as a trophic factor for several distinct populations of neurons. *Proc. Natl. Acad. Sci. USA* **83**, 2714–2718 (1986).
- Tuszynski, M. H. *et al.* A phase 1 clinical trial of nerve growth factor gene therapy for Alzheimer disease. *Nat. Med.* **11**, 551–555 (2005).

3. Gall, C. M. Seizure-Induced Changes in Neurotrophin Expression: Implications for Epilepsy. *Exp. Neurol.* **124**, 150–166 (1993).
4. Meghan, C. B. *et al.* Regulatory effect of nerve growth factor in $\alpha\beta 1$ integrin-dependent progression of glioblastoma. *Neuro. Oncol.* **10**, 968–980 (2008).
5. Dollé, L. *et al.* Nerve growth factor overexpression and autocrine loop in breast cancer cells. *Oncogene.* **22**, 5592–5601 (2003).
6. Descamps, S. *et al.* Nerve Growth Factor Stimulates Proliferation and Survival of Human Breast Cancer Cells through Two Distinct Signaling Pathways. *J. Biol. Chem.* **276**, 17864–17870 (2001).
7. Greene, L. A. & Tischler, A. S. Establishment of a noradrenergic clonal line of rat adrenal pheochromocytoma cells which respond to nerve growth factor. *Proc. Natl. Acad. Sci. USA* **73**, 2424–2428 (1976).
8. Chao, M. Neurotrophin receptors: a window into neuronal differentiation. *Neuron.* **9**, 583–593 (1992).
9. Huang, E. J. & Reichardt, L. F. Trk receptors: Roles in Neuronal Signal Transduction. *Annu. Rev. Biochem.* **72**, 609–642 (2003).
10. Klesse, L. J. *et al.* Nerve growth factor induces survival and differentiation through two distinct signaling cascades in PC12 cells. *Oncogene.* **18**, 2055–2068 (1999).
11. Cowley, S. *et al.* Activation of MAP kinase kinase is necessary and sufficient for PC12 differentiation and for transformation of NIH 3T3 cells. *Cell.* **77**, 841–852 (1994).
12. Li, J. W. & Vederas, J. C. Drug discovery and natural products: end of an era or an endless frontier? *Science.* **325**, 161–165 (2009).
13. Huang, J. M. *et al.* Structure and Neurotrophic Activity of *seco*-Prezizaane-Type Sesquiterpenes from *Illicium merrillianum*. *J. Nat. Prod.* **64**, 428–431 (2001).
14. Kuroyanagi, M. *et al.* Neurite outgrowth-promoting active constituents of the Japanese cypress (*Chamaecyparis obtusa*). *Chem. Pharm. Bull.* **56**, 60–63 (2008).
15. Huang, J. M. *et al.* Brine Shrimp Lethality Test Active Constituents and New Highly Oxygenated *Seco*-prezizaane-Type Sesquiterpenes from *Illicium merrillianum*. *Chem. Pharm. Bull.* **50**, 133–136 (2002).
16. Huang, J. M. *et al.* Merrilactone A, a novel neurotrophic sesquiterpene dilactone from *Illicium merrillianum*. *Tetrahedron Lett.* **41**, 6111–6114 (2000).
17. Liu, Y. H. *et al.* Menispermaceae Magnoliaceae. *Flora Republicae Popularis Sinicae.* **30**, 227–228 (Science Press, Beijing, 1996).
18. Tian, X. H. *et al.* Merrilliadione, a rare isopropyl (13→11)-*abeo*-9,11-*seco* abietane diterpene from *Illicium merrillianum*. *Eur. J. Org. Chem.* **22**, 4753–4758 (2014).
19. Berova, N., Bari, L. D. & Pescitelli, G. Application of electronic circular dichroism in configurational and conformational analysis of organic compounds. *Chem. Soc. Rev.* **36**, 914–931 (2007).
20. Gao, Y. P. *et al.* Incarvilleatone, a Unique Benzofuranone Dimer from *Incarvillea younghusbandii* and Its Inhibition against Nitric Oxide (NO) Release. *Org. Lett.* **14**, 1954–1957 (2012).
21. Shi, X. W. *et al.* Cyathane diterpenes from Chinese mushroom *Sarcodon scabrosus* and their neurite outgrowth-promoting activity. *Eur. J. Med. Chem.* **46**, 3112–3117 (2011).
22. Liu, L. *et al.* Scabronine M, a novel inhibitor of NGF-induced neurite outgrowth from PC12 cells from the fungus *Sarcodon scabrosus*. *Bioorg. Med. Chem. Lett.* **22**, 2401–2406 (2012).
23. Zhang, W. & Liu, H. T. MAPK signal pathways in the regulation of cell proliferation in mammalian cells. *Cell Res.* **12**, 9–18 (2002).
24. Brunet, A., Datta, S. R. & Greenberg, M. E. Transcription-dependent and -independent control of neuronal survival by the PI3K-Akt signaling pathway. *Curr. Opin. Neurobiol.* **11**, 297–305 (2001).
25. Franke, T. F. *et al.* PI3K/Akt and apoptosis: size matters. *Oncogene.* **22**, 8983–8998 (2003).

Acknowledgements

The work was supported by the following programs: NSFC (81373301, 81230090, 1302658), Shanghai Leading Academic Discipline Project (B906), Shanghai Engineering Research Center for the Preparation of Bioactive Natural Products (10DZ2251300), Scientific Foundation of Shanghai, China (12401900801, 13401900101) and the National Key Technology R&D Program of China (2012BAI29B06).

Author Contributions

Z.W.D., S.Y.H. and T.X.H. designed the phytochemical, computational and biological experiments. T.X.H. conducted the phytochemical experiments. Y.R.C., T.X.H., Z.H.W. and S.L. conducted the biological experiments. L.H.L. and H.W.W. conducted the quantum mechanical computation of electronic circular dichroism. T.X.H. analyzed the above data and wrote the paper.

Additional Information

Supplementary information accompanies this paper at <http://www.nature.com/srep>

Competing financial interests: The authors declare no competing financial interests.

How to cite this article: Tian, X. *et al.* Distinctive effect on nerve growth factor-induced PC12 cell neurite outgrowth by two unique neolignan enantiomers from *Illicium merrillianum*. *Sci. Rep.* **5**, 16982; doi: 10.1038/srep16982 (2015).



This work is licensed under a Creative Commons Attribution 4.0 International License. The images or other third party material in this article are included in the article's Creative Commons license, unless indicated otherwise in the credit line; if the material is not included under the Creative Commons license, users will need to obtain permission from the license holder to reproduce the material. To view a copy of this license, visit <http://creativecommons.org/licenses/by/4.0/>